Hindawi
Journal of Spectroscopy
Volume 2020, Article ID 8730471, 7 pages
https://doi.org/10.1155/2020/8730471

Research Article

Effect of Absorption and Scattering on Fluorescence of Buried Tumours

Kawthar M. K. Alghourani,[1] Wesam Bachir ,[1,2] and George Karraz[2]

[1]*Biomedical Photonics Laboratory, Higher Institute for Laser Research and Applications, Damascus University, Damascus, Syria*
[2]*Faculty of Informatics Engineering, Al-Sham Private University, Damascus, Syria*

Correspondence should be addressed to Wesam Bachir; wesambachir002@gmail.com

Received 10 January 2020; Revised 13 February 2020; Accepted 25 February 2020; Published 19 March 2020

Academic Editor: Daniel Cozzolino

Fluorescence spectroscopy is widely used for biomedical optical diagnosis and surgical resection of tumours. This work investigates laser-induced fluorescence spectroscopy of fluorescence inclusions that are embedded in turbid media. 405 nm laser diode is used for exciting buried protoporphyrin- (PpIX) based inclusions in brain-like optical phantoms. Effects of scattering and absorption of the turbid medium on the recorded fluorescence signal and depth-resolved fluorescence were studied. Results show that optical properties of the surrounding turbid medium influence the intensity of the fluorescence signal. Absorption coefficient of the surrounding medium is the major contributor to the fluorescent signal. Analysis of the recorded fluorescence spectra shows that the effect of absorption coefficient is larger than the effect of scattering coefficient on the fluorescence intensity by nearly fivefold. The findings indicate that the fluorescence signal could be used as a biomarker of optical property variations through different stages of malignancy. This can enhance the detectability of malignant tissue for diagnostic and surgical purposes as well.

1. Introduction

Surgical removal of tumour mass is the most commonly used approach in the management of cancer [1]; however, precision and effectiveness of these procedures have increasingly become challenging in medicine [2]. Locations of tumours might be determined intraoperatively by visual inspection under bright light and information provided by advanced surgical navigation systems including computed tomography (CT), magnetic resonance imaging (MRI), and intraoperative ultrasound [3]. However, the accuracy of these conventional imaging techniques is not adequate for localizing tumours and buried tumours in particular [4]. Therefore, there is a pressing need for the development of an effective tool that allows intraoperative detection of embedded tumours with high sensitivity and specificity. Over the past two decades, there has been a growing interest in optical measurements for tumour localization owing to its safety and efficiency [5]. Several optical spectroscopy-based techniques have been developed and tested to meet this need [6]. Fluorescence spectroscopy is one of the promising optical modalities for this purpose [7]. It is a noninvasive technique in terms of excitation and detecting the remitted signal on the surface. The measured signal contains information about the concentration and the location of the target fluorophores of interest with which functional and physiological characteristics of the underlying tissue can be quantitatively determined. Thus, fluorescence spectroscopy provides a potential optical technique for discriminating healthy and tumour tissues [8].

Fluorescence spectroscopy has been highly developed for tumour surgery using the optical contrast provided by protoporphyrin IX (PpIX) that is endogenously synthesized in tumour cells following administration of the prodrug δ-aminolevulinic acid (ALA), whereas PpIX is a natural substance in the heme cycle which is rapidly eliminated from the tissue [9]. Laser wavelength at 405 nm is absorbed by protoporphyrin IX. The molecules of PpIX re-emit the fluorescence spectrum with pronounced peaks at 635 nm and 704 nm [10]. Therefore, protoporphyrin IX (PpIX) is a

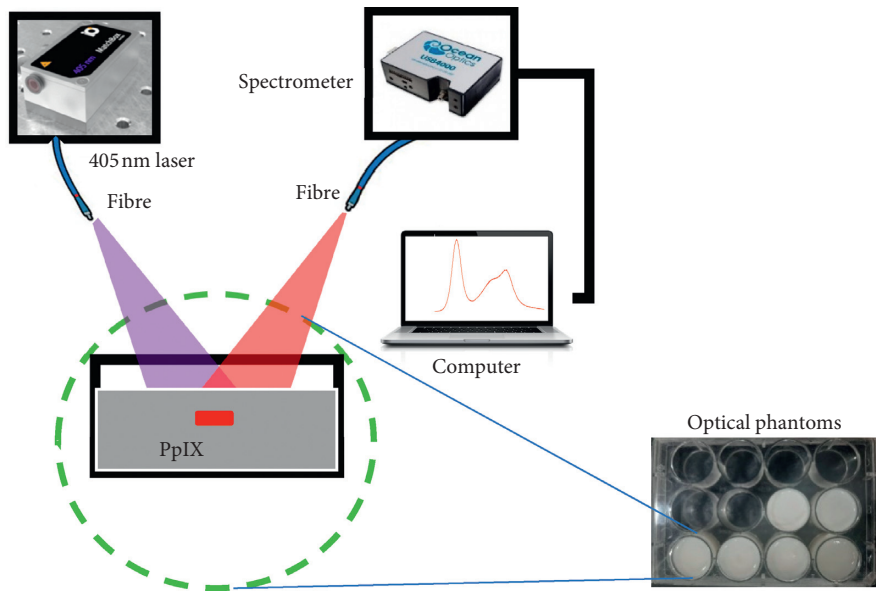

Figure 1: Overview of the optical setup used for recording fluorescence spectra emanated from buried fluorescence inclusions in the brain tissue-like optical phantom.

photosensitizer and fluorophore of interest both for experimental photo-based therapies and for diagnostic assessment of suspicious tissue during surgery [11].

Nonetheless, much of the previous research has focused on developing optical methods for superficial tumours in order to delineate the borders between normal and cancerous tissue during tumour resection [12]. In contrast, a few studies have investigated the fluorescence spectroscopy for subsurface tumours and the effect of medium's optical potteries of the fluorescence signal. Swartling et al. [13] studied the spectral changes of the fluorescence signal emanated from the subsurface fluorescence layer in an optical phantom. Modelling of spectral changes using Monte Carlo due to embedded fluorescent inclusions has also been investigated by Svensson and Andersson-Engels [14]. More recently, macroscopic optical imaging techniques have been devised for estimating the fluorescence depth in the optically tissue-mimicking turbid medium [15] as a 635 nm laser diode was used for excitation.

To the best of our knowledge, the effect of the surrounding optical properties on the detected fluorescence from subsurface tumours has not been thoroughly investigated; hence, the independent effect of optical coefficients need not be independently quantified.

The aim of the present work is to experimentally investigate depth-resolved fluorescence spectroscopy in tissue-simulating optical phantoms containing embedded PpIX-based fluorescent inclusions located at different depths under the surface. Effect of absorption and scattering coefficients on the fluorescence signal is discussed.

2. Materials and Methods

A schematic drawing representing the optical instrumentation for fluorescence measurements is depicted in Figure 1. Fluorescence inclusion was made of a cylindrical plastic tube filled with PpIX solution with a concentration of 3 mg/mL. The cylindrical inclusion has a length of 5 mm and diameter of 2 mm. The inclusions were buried in the turbid medium at different depths. All optical phantoms in this study were arranged in the 12-well microwell.

The light source was 405 nm fibre-coupled diode laser (0405 nm 13A, Integrated Optics Inc. Lithuania), and laser power was delivered to the sample in the CW mode with a power of 20 MW. For collecting the emitted fluorescence signal, a collection fibre (Ocean Optics Inc.) with a diameter of 400 μm was used. The fibre is coupled to a miniature spectrometer (USB4000, Ocean Optics Inc. USA). The spectrometer is connected via an USB cable to the computer for acquiring fluorescence spectra. Recoding data and signal processing of the collected spectra were controlled by SpectraSuit software (Ocean Optics Inc., 2011).

Two main sets of optical phantoms mimicking the optical properties of biological tissues were investigated in order to quantify the effect of optical properties on fluorescent intensity. The optical properties were defined to cover the corresponding values of healthy and cancerous brain tissue. For the effect of absorption coefficient of the surrounding medium, four sets of phantoms were built. The values of absorption coefficient ranged between 0.5 and 2 mm^{-1}. For each one of the absorption coefficient values, a subset of 5 optical phantoms was fabricated corresponding to five depths of the PpIX inclusion, that is, 1, 3, 5, 7, and 10 mm. Similarly, for quantifying the scattering effect of the surrounding medium, another four sets of optical phantoms were constructed. The values of scattering coefficient ranged between 10 and 50 mm^{-1}. For each one of the scattering coefficient values, a subset of 5 optical phantoms was fabricated corresponding to five depths of the PpIX inclusion, that is, 1, 3, 5, 7, and 10 mm.

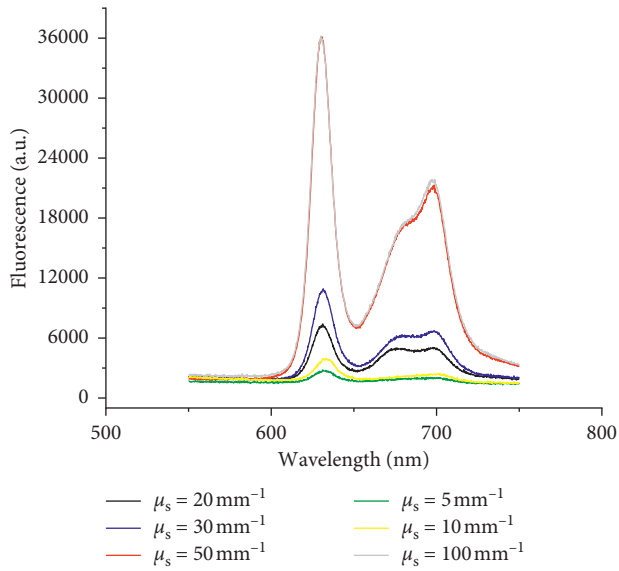

Figure 2: Recordings of fluorescence spectra for different values of scattering coefficient.

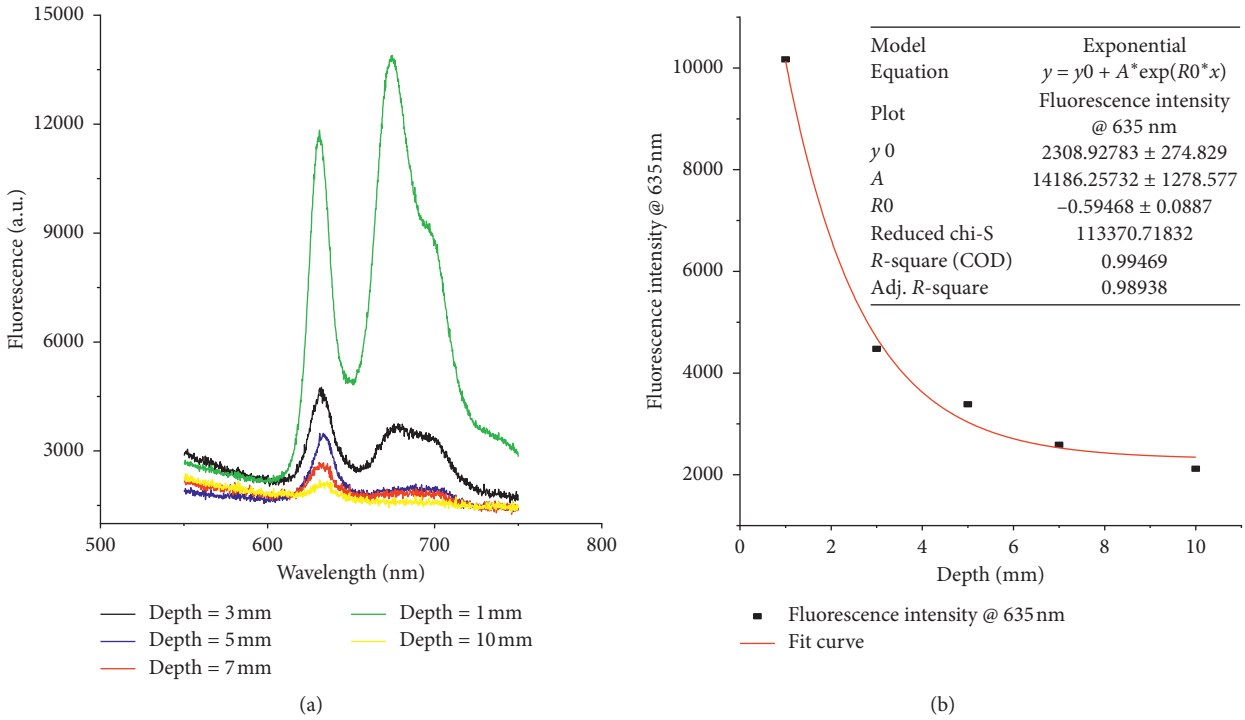

Figure 3: (a) Recordings of fluorescence spectra for different depths of the PpIX inclusion. (b) Fluorescence intensity at 635 nm for different depths of the PpIX inclusion in the optical phantom. Fitted curve shows exponential behaviour of the fluorescence intensity as a function of the depth.

3. Results and Discussion

All PpIX inclusion fluorescence measurements were carried out in dark laboratory setting. As a preliminary measurement, five scattering coefficient values ranged from 1 to 100 mm^{-1} were constructed and arranged in a microwell followed by measuring the fluorescence spectra of the embedded inclusion. Figure 2 shows the fluorescence spectra for different values of scattering coefficient.

The intensity of the fluorescent signal is directly proportional to the scattering power of the optical phantom. It can be seen from Figure 2 that the intensity of fluorescence for 50 and 100 mm^{-1} is approximately the same. That is, the fluorescence signal may reach a saturation level for higher

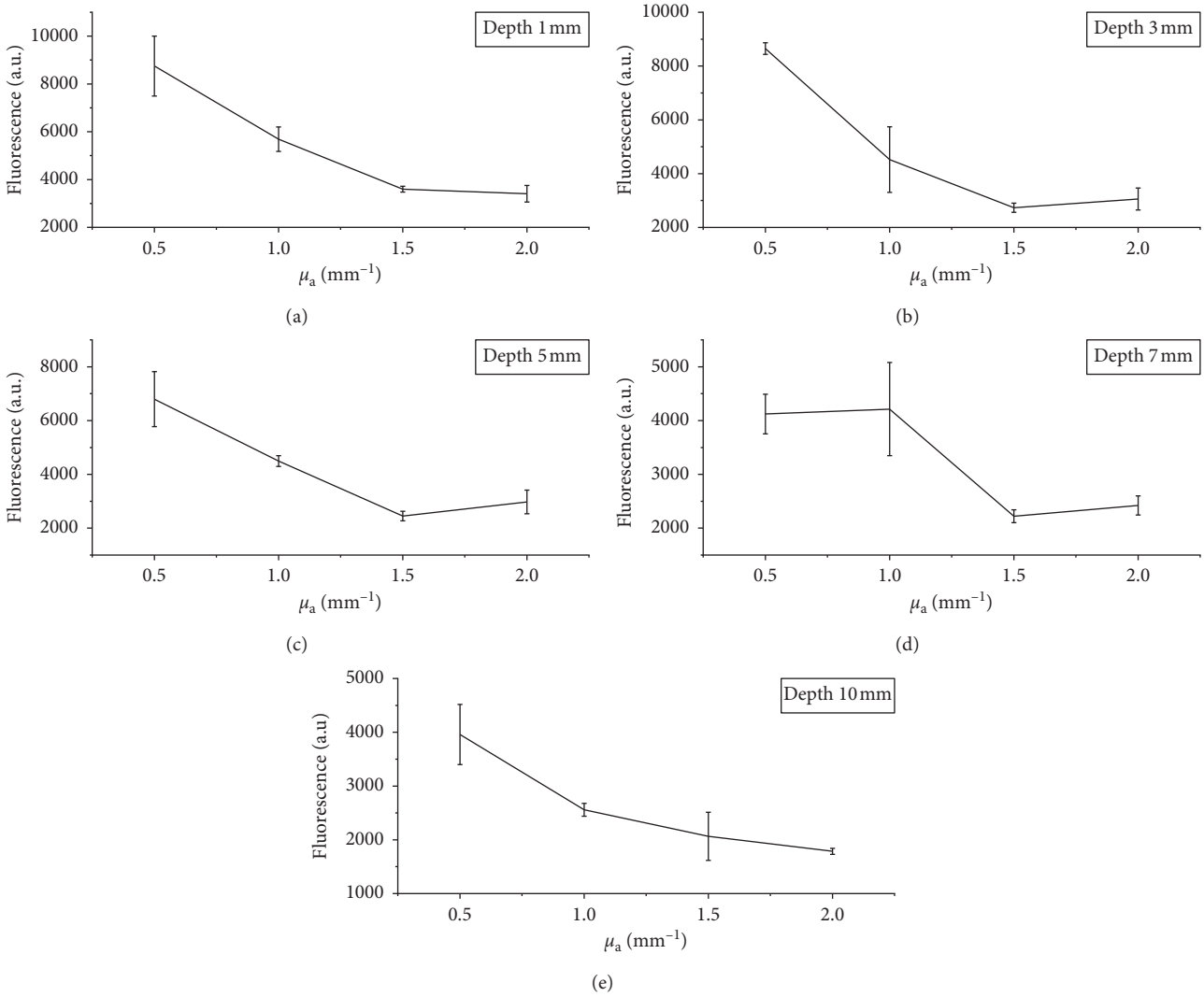

Figure 4: (a–e) Mean values and standard deviations of fluorescence intensity at 635 nm as a function of absorption coefficient for different depths.

values of the scattering coefficient. Figure 3(a) shows the fluorescence detected for different depths of the PpIX inclusion inside the optical phantom. The depth of inclusion ranged from 1 mm to 10 mm. In this case, one can notice that the fluorescence intensity is inversely proportional to the depth. This decline in intensity can be fitted to the exponential curve as displayed in Figure 3(b).

All PpIX fluorescence spectra showed distinctive peaks at 635 and 704 nm, and thus, fluorescence intensity values at these specific wavelengths were used in further analysis of the measured spectra. Mean values and standard deviation of fluorescence intensities are plotted for different depths and for a range of absorption coefficients (from 0.5 to 2 mm^{-1}) as can be seen in Figures 4(a)–4(e). All produced curves show noticeable decline in fluorescence intensity for all studied depths. This decrease in fluorescence intensity can be explained by the decrease in the number of photons reaching the PpIX inclusion due to absorption.

In addition, mean values and standard deviation of fluorescence intensities are plotted for different depths and for a range of scattering coefficients (from 10 to 50 mm^{-1}) as presented in Figures 5(a)–5(e)). All produced curves show marked increase in fluorescence intensity for all investigated depths of PpIX inclusion. This increase in the fluorescence signal can be attributed to the increased number of photons exciting the PpIX inclusion due to scattering.

It is noteworthy to say that all curves in Figures 4 and 5 show nonlinear behaviour of fluorescence variation as a function of absorption and scattering coefficients. This is in agreement with prior studies [16].

In a study conducted by Markwardt et al. [17], the effect of photobleaching on the recorded fluorescence signals was avoided by limiting the excitation time. In this study, each optical phantom contained a cylindrical inclusion that had been excited with a set length of excitation time; hence, the effect of photobleaching is standardized for all samples.

Furthermore, it is of great importance to quantify the effect of variation in optical properties on the recorded fluorescence signal. To achieve that, the variation effects of scattering and absorption were analysed independently.

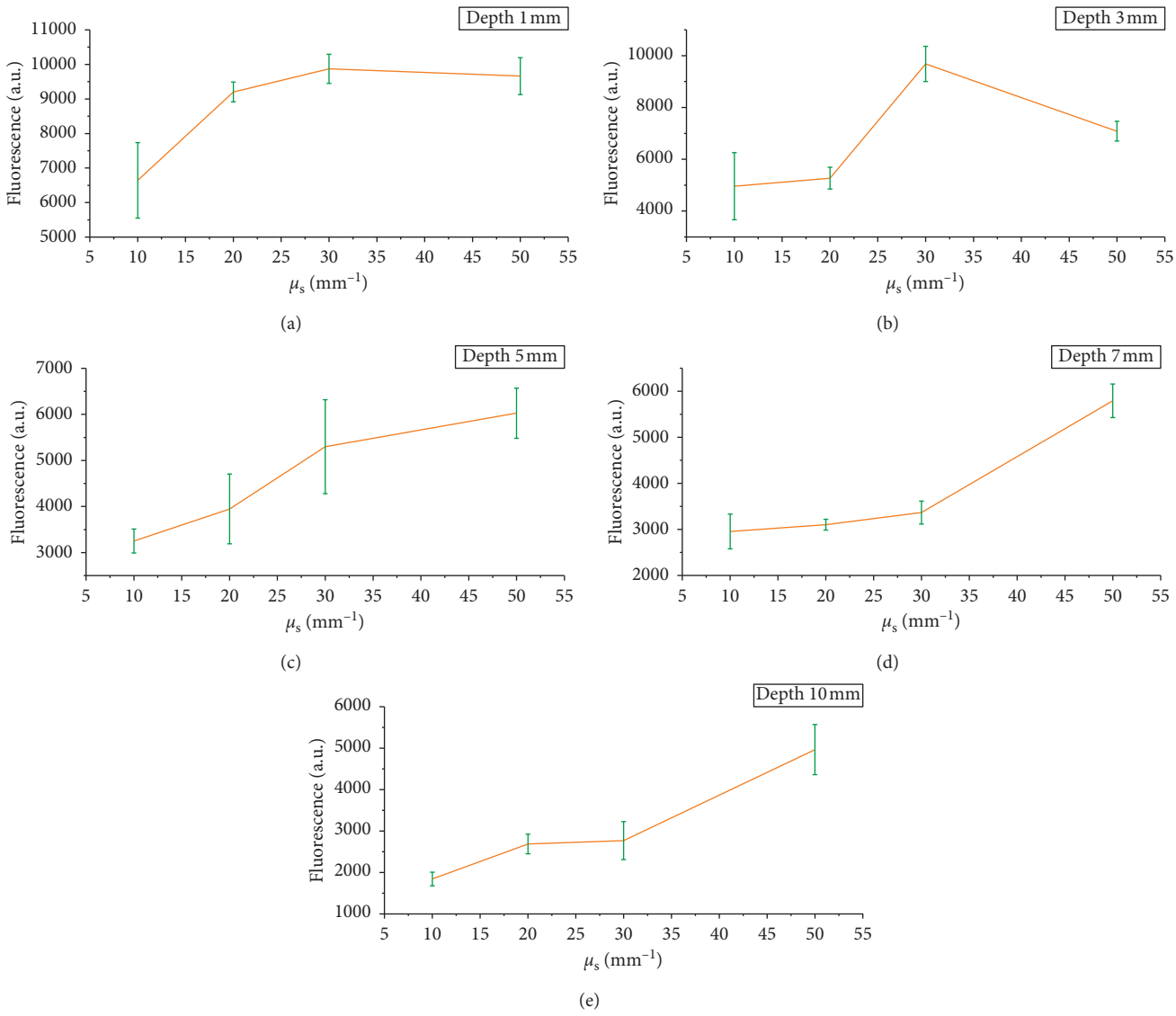

Figure 5: (a–e) Mean values and standard deviations of fluorescence intensity at 635 nm as a function of scattering coefficient for different depths.

First, for absorption coefficient, attenuation in fluorescence intensity at 635 nm over the abovementioned range of absorption coefficients was calculated for each depth based on the following equation:

$$\text{Variation}_{\mu_a,d} = \frac{F_{\text{abs}_{\mu_a\,(\max)}} - F_{\text{abs}_{\mu_a\,(\min)}}}{F_{\text{abs}_{\mu_a\,(\max)}}} \times 100\%, \quad (1)$$

where $\text{Variation}_{\mu_a,d}$ is the variation in intensity at 635 nm for a given depth of the PpIX inclusion, $F_{\text{abs}_{\mu_a\,(\max)}}$ is the fluorescence intensity in the absorbing medium with the maximum absorption coefficient used in this study, that is, corresponding to the value of 2 mm^{-1}, and $F_{\text{abs}_{\mu_a\,(\min)}}$ is the fluorescence intensity in the absorbing medium with the minimum absorption coefficient used in this study, that is, corresponding to the value of 0.5 mm^{-1}. The variation percentages for absorption are presented in Figure 6(a).

Second, for scattering coefficient, elevation in fluorescence intensity at 635 nm over the abovementioned range of scattering coefficients was calculated for each depth as expressed by the following equation

$$\text{Variation}_{\mu_s,d} = \frac{F_{\text{scat}_{\mu_s\,(\max)}} - F_{\text{scat}_{\mu_s\,(\min)}}}{F_{\text{scat}_{\mu_s\,(\max)}}} \times 100\%, \quad (2)$$

where $\text{Variation}_{\mu_s,d}$ is the variation in intensity at 635 nm for a given depth of the PpIX inclusion, $F_{\text{scat}_{\mu_s\,(\max)}}$ is the fluorescence intensity in the scattering medium with the maximum scattering coefficient used in this study, that is, corresponding to the value of 50 mm^{-1}, and $F_{\text{scat}_{\mu_s\,(\min)}}$ is the fluorescence intensity in the scattering medium with the minimum scattering coefficient used in this study, that is, corresponding to the value of 10 mm^{-1}. Figure 6(a) displays the variation percentages due to scattering for all depths.

Overall quantification of variation can be evaluated by taking the average value for all corresponding depths as shown in Figure 6(b).

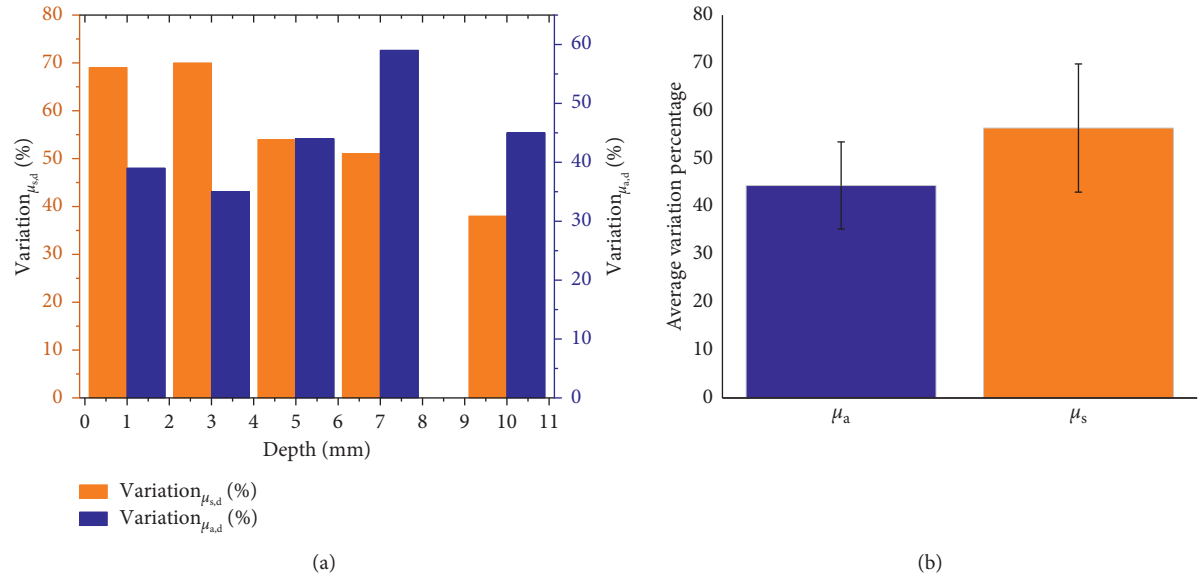

Figure 6: (a) Variation in fluorescence intensity at 635 nm due to scattering and absorption for different depths. (b) Average variation percentage over all depths for scattering and absorption.

It can be clearly noticed that both variations for absorption and scattering are comparable (44% for absorption vs. 55% for scattering). However, the corresponding ranges for scattering and absorption coefficients are different. Thus, we can say that the effect of absorption coefficient of the medium on the measured fluorescence has far greater than the effect of the scattering coefficient. In other words, fluorescence spectra for embedded inclusions are more sensitive to the variation in absorption coefficient.

Taking into account the nonlinear trend of the variation in fluorescence intensity for both scattering and absorbing media, the relationship between fluorescence intensity and optical properties can be transformed to a linear one by taking the logarithm of the measured quantity, i.e., the recorded fluorescence. As a result, we deduce that the logarithm of fluorescence intensity is inversely proportional to the change in absorption coefficient, and likewise, the logarithm of fluorescence intensity is directly proportional to the change in scattering coefficient. Consequently, based on ranges in optical properties used in this study, an increment of 1 mm^{-1} in absorption coefficient leads to decrease in fluorescence intensity by 18%. In contrast, an increment in scattering coefficient of 1 mm^{-1} corresponds to increase in the fluorescence signal by 4%. That is to say, the effect of absorption coefficient is larger than the effect of scattering coefficient on the fluorescence intensity by nearly fivefold.

Stepp et al. [18] measured the optical properties of brain tissue through different stages of tumour development in rats, and they found that absorption coefficient is largely affected over the development process of tumours. This indicates that the fluorescence signal could be used as a biomarker of optical property variations through different stages of malignancy.

Analytical method for estimating the depth of fluorescence inclusions was also derived [19]. This method requires prior knowledge of optical properties of the turbid medium. However, in clinical applications, fluorescence concentration and optical properties are unknown and hence the potential contribution of this study in correlating the fluorescence intensity with optical properties.

Another area for future work could take into account other excitation wavelengths that are being used [20] for exciting biological fluorophores.

One possible limitation of the presented work was the noticed deviations in the fluorescence signal in both absorption and scattering measurements. This can be explained by the unavoidable error in positioning the fibre probe over the optical phantom. However, the effect of this setback on the overall results can be negligible.

4. Conclusions

This paper attempted to experimentally evaluate the effect of optical properties of the medium on the depth-resolved measured fluorescence emanated from PpIX-filled inclusions. The results reveal that absorption coefficient has far greater effect on the intensity of fluorescence than the scattering coefficient. Embedded fluorescence inclusions therefore are more sensitive to variations in absorption coefficients of the surrounding medium. This has profound implications in biomedical optical measurements of embedded tumours like brain tumours that contain certain concentration of PpIX and surrounded by biological tissue of varying optical properties. This study can also be extended to investigate other optical properties associated with different biological tissues and this in turn would improve the accuracy of biomedical optical diagnostics.

Data Availability

The data used to support the findings of this study are available from the corresponding author upon request.

Conflicts of Interest

The authors declare that there are no conflicts of interest regarding the publication of this paper.

Acknowledgments

This work was funded by Damascus University.

References

[1] W. Stummer, H.-J. Reulen, T. Meinel et al., "Extent of resection and survival in glioblastoma multiforme: identification of and adjustment for bias," *Neurosurgery-online*, vol. 62, pp. 564–576, 2008.

[2] J. Drappatz, A. D. Norden, and P. Y. Wen, "Therapeutic strategies for inhibiting invasion in glioblastoma," *Expert Review of Neurotherapeutics*, vol. 9, no. 4, pp. 519–534, 2009.

[3] L. C. Hou, A. Veeravagu, A. R. Hsu, and V. C. K. Tse, "Recurrent glioblastoma multiforme: a review of natural history and management options," *Neurosurgical Focus*, vol. 20, no. 4, p. E3, 2006.

[4] A. Claes, A. J. Idema, and P. Wesseling, "Diffuse glioma growth: a guerilla war," *Acta Neuropathologica*, vol. 114, no. 5, pp. 443–458, 2007.

[5] J. C. O. Richter, N. Haj-Hosseini, M. Hallbeck, and K. Wårdell, "Combination of hand-held probe and microscopy for fluorescence guided surgery in the brain tumor marginal zone," *Photodiagnosis and Photodynamic Therapy*, vol. 18, pp. 185–192, 2017.

[6] P. A. Valdés, A. Kim, F. Leblond et al., "Combined fluorescence and reflectance spectroscopy for in vivo quantification of cancer biomarkers in low and high-grade glioma surgery," *Journal of Biomedical Optics*, vol. 16, no. 11, Article ID 116007, 2011.

[7] B. W. Pogue, T. C. Zhu, V. Ntziachristos et al., "Fluorescence-guided surgery and intervention—an AAPM emerging technology blue paper," *Medical Physics*, vol. 45, no. 6, pp. 2681–2688, 2018.

[8] K. Paulsen, N. Ikeda, N. Nonoguchi et al., "Enhanced expression of coproporphyrinogen oxidase in malignant brain tumors: CPOX expression and 5-ALA-induced fluorescence," *Neuro-Oncology*, vol. 13, no. 11, pp. 1234–1243, 2011.

[9] J. Kajimoto, J. T. H. M. Van Den Akker, P. Juzenas et al., "On the basis for tumor selectivity in the 5-aminolevulinic acid-induced synthesis of protoporphyrin IX," *Journal of Porphyrins and Phthalocyanines*, vol. 5, no. 2, pp. 170–176, 2001.

[10] M. B. Ericson, S. Grapengiesser, F. Gudmundson et al., "A spectroscopic study of the photobleaching of protoporphyrin IX in solution," *Lasers in Medical Science*, vol. 18, no. 1, pp. 56–62, 2003.

[11] J. C. O. Wennberg, N. Haj-Hosseini, S. Andersson-Engel, and K. Wårdell, "Fluorescence spectroscopy measurements in ultrasonic navigated resection of malignant brain tumors," *Lasers in Surgery and Medicine*, vol. 43, no. 1, pp. 8–14, 2011.

[12] J. T. Elliott, A. V. Dsouza, S. C. Davis et al., "Review of fluorescence guided surgery visualization and overlay techniques," *Biomedical Optics Express*, vol. 6, no. 10, pp. 3765–3782, 2015.

[13] J. Swartling, J. Svensson, D. Bengtsson, K. Terike, and S. Andersson-Engels, "Fluorescence spectra provide information on the depth of fluorescent lesions in tissue," *Applied Optics*, vol. 44, no. 10, pp. 1934–1941, 2005.

[14] J. Svensson and S. Andersson-Engels, "Modeling of spectral changes for depth localization of fluorescent inclusion," *Optics Express*, vol. 13, no. 11, p. 4263, 2005.

[15] K. K. Kolste, S. C. Kanick, P. A. Valdés et al., "Macroscopic optical imaging technique for wide-field estimation of fluorescence depth in optically turbid media for application in brain tumor surgical guidance," *Journal of Biomedical Optics*, vol. 20, no. 2, Article ID 026002, 2015.

[16] A. Kim, M. Khurana, Y. Moriyama, and B. C. Wilson, "Quantification of in vivo fluorescence decoupled from the effects of tissue optical properties using fiber-optic spectroscopy measurements," *Journal of Biomedical Optics*, vol. 15, no. 6, Article ID 067006, 2010.

[17] N. A. Markwardt, N. Haj-Hosseini, B. Hollnburger, H. Stepp, P. Zelenkov, and A. Rühm, "405 nm versus 633 nm for protoporphyrin IX excitation in fluorescence-guided stereotactic biopsy of brain tumors," *Journal of Biophotonics*, vol. 9, no. 9, pp. 901–912, 2016.

[18] E. A. Stepp, A. N. Bashkatov, D. K. Tuchina et al., "Optical properties of brain tissues at the different stages of glioma development in rats: pilot study," *Biomedical Optics Express*, vol. 10, no. 10, pp. 5182–5197, 2019.

[19] A. Dyachenko, A. Da Silva, M. Berger, J. Boutet, J.-M. Dinten, and A. C. Boccara, "Analytical method for localizing a fluorescent inclusion in a turbid medium," *Applied Optics*, vol. 46, no. 11, pp. 2131–2137, 2007.

[20] D. Wirth, K. Kolste, S. Kanick, D. W. Roberts, F. Leblond, and K. D. Paulsen, "Fluorescence depth estimation from wide-field optical imaging data for guiding brain tumor resection: a multi-inclusion phantom study," *Biomedical Optics Express*, vol. 8, no. 8, p. 3656, 2017.